Supplementary methods and results

GABRIEL campaign in the Guyanas

In October 2005, 10 measurement flights were performed over Suriname, Guyana, French Guyana and the adjacent tropical Atlantic Ocean within the GABRIEL Campaign (Guyanas Atmosphere-Biosphere exchange and Radicals Intensive Experiment with the Learjet; see http://www.mpch-mainz.mpg.de/~scheeren/gabriel/). The area investigated (Figure S1) is largely covered by primary rain forest, and has a low average population density of about 3/km^2, mostly concentrated along the Atlantic coast.

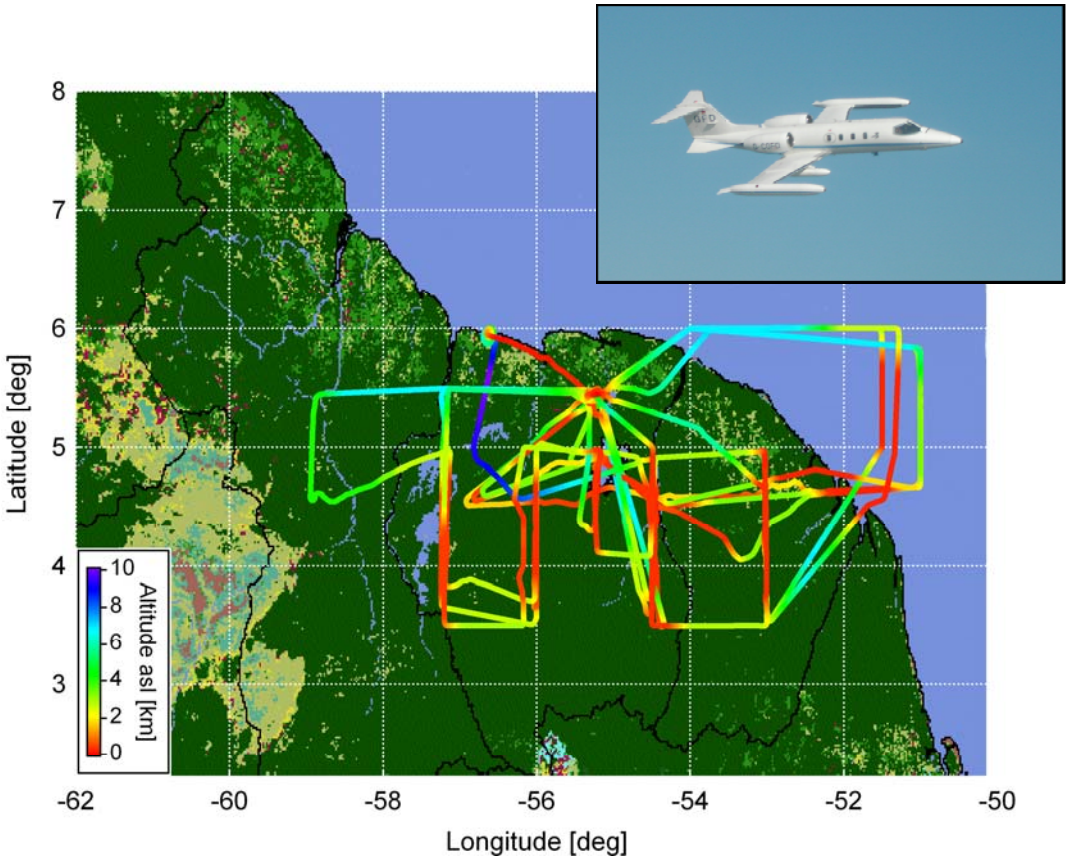

Figure S1. Measurement flight tracks and altitude during the GABRIEL campaign in October 2005, using a Learjet 35A (insert).

Figure S1 shows the flight tracks of our instrumented Learjet 35A over an area of about 0.2 Mkm^2. Campaign support was provided by the Gesellschaft für Flugzieldarstellung, Hohn, Germany (flight operations); Enviscope GmbH, Frankfurt, Germany (technical and logistical support); Suriname Meteorological Service, Paramaribo; Royal Netherlands Meteorological Institute, De Bilt (meteorological support); Anton de Kom University of Suriname, Paramaribo; and the Foundation for Nature Conservation in Suriname. Table S1 lists the aircraft instrumentation and measurement uncertainties. For additional information and references we refer to Colomb et al. (2007), Fischer et al. (2006), Stickler et al. (2006, 2007) and Williams et al. (2007).

The GABRIEL campaign was a continuation of the Cooperative LBA (Large-scale Biosphere-Atmosphere) Regional Experiment (CLAIRE), which included an aircraft measurement campaign in March 1998 (Crutzen et al., 2000; Andreae et al., 2001; Formenti et al., 2001; Pöschl et al., 2001; Warneke et al., 2001; Williams et al., 2001a,b). In the LBA-CLAIRE period in March the inter-tropical convergence zone (ITCZ) was located south of the measurement area, and the results represent the tropical troposphere in the meteorological Northern Hemisphere (Peters et al., 2004).

In October 2005 the ITCZ was located to the north, and the measurements are representative of the same tropical region in the meteorological Southern Hemisphere. One of the interesting aspects of the Guyanas is that the ITCZ migrates across two times per year. In December-January and May-July the ITCZ is located directly over the area, associated with about 150-200 and 300 mm/month precipitation, respectively. In the relatively dry periods March-April and August-November precipitation rates are typically 150 and 100-150 mm/month, respectively (Nurmohamed and Naipal, 2006).

Table S1. GABRIEL measurement instrumentation on the Learjet aircraft. Note that accuracy represents the total uncertainty.

Parameter	Measurement technique	Detection limit	Precision	Accuracy
CO	Quantum cascade laser spectrometry	0.2 ppbv		2.5%
CH_2O	Quantum cascade laser spectrometry	0.25 ppbv	25%	27%
H_2O_2	Derivatisation and enzyme fluorescence	0.029 ppbv	10%	15%
ROOH	Derivatisation and enzyme fluorescence	< 0.029 ppbv	< 10%	26%
OH	Laser-induced fluorescence	0.02 pptv	7%	<40%
HO_2	Laser-induced fluorescence	0.07 pptv	1%	<60%
NO	Chemiluminescence	5 pptv		12%
O_3	Chemiluminescence	2 ppbv		2%
$J(NO_2)$	Filter radiometry		1%	10%
CH_3OH	Proton transfer reaction mass spectrometry	0.269 ppbv	39%	40%
CH_3CN	Proton transfer reaction mass spectrometry	0.068 ppbv	20%	22%
$CH_3C(O)CH_3$	Proton transfer reaction mass spectrometry	0.094 ppbv	17%	20%
Isoprene	Proton transfer reaction mass spectrometry	0.099 ppbv	7%	12%
Methyl-vinyl ketone	Proton transfer reaction mass spectrometry	0.093 ppbv	12%	16%
H_2O	Infrared absorption spectrometry	200 ppm		5%
CO_2	Infrared absorption spectrometry			0.3 ppmv

GABRIEL meteorology

The position of the ITCZ is associated with the sea surface temperature (SST) difference between the tropical North and South Atlantic Oceans, and during August-November the north-south SST gradient is relatively steep. Consequently, during the GABRIEL campaign in October 2005, the southeasterly trade winds were fairly strong, typically about 5 m/s and the aircraft measurements and balloon soundings from Paramaribo show that these wind conditions were almost constant up to about 8 km and occasionally up to 12-14 km altitude. Further aloft, weak westerly winds prevailed. For this reason our present analysis focuses on the troposphere up to 8 km altitude. The frequency of isolated thunderstorms and rain showers in the late afternoon during GABRIEL was approximately once every three days.

The cumulonimbus frequency was highest in mid-October under the influence of a westward travelling tropical wave and a cross-equatorial upper level trough after 10 October. The atmospheric boundary layer (BL) over the rainforest, defined by sensible and latent heating, was shallow at night (several hundred metres), while during the afternoon cumulus clouds developed a convective boundary layer (or mixed layer) up to about 2-3 km altitude. The mean BL height, as defined by vertical gradients of chemical constituents during daylight (mixing layer) was about 1 km over the ocean and 1.5 km over land. High resolution balloon soundings in the forest (performed in October 2006) showed that up to about 12 am local time the BL top was well-defined by a temperature inversion, whereas later in the afternoon the growth of cumulus clouds eliminated the inversion and the BL was ill-defined. The relative humidity in the BL was typically 70-90%, decreasing rapidly with altitude in the free troposphere.

Isoprene photo-oxidation

In the atmosphere the lifetime of the C_5 diolefin isoprene is largely determined by the reaction with OH radicals. Reactions with O_3 and NO_3 radicals are minor loss processes. In general terms the oxidation of isoprene is described by alkene chemistry; however, the chemistry is highly complex and has been studied mostly for high-NO conditions because of the importance in photochemical ozone formation in polluted environments (Paulson et al., 1992; Miyoshi et al., 1994; Carter and Atkinson, 1996; Pinho et al., 2005).

The OH adds to one of the double bonds of isoprene, forming alkyl radicals (R) that in turn add O_2 to form peroxy radicals (RO_2)

Isoprene + OH → R,

$R + O_2 \rightarrow RO_2$.

In high-NO conditions, typically at NO > 50 pptv, the RO_2 radicals decompose by converting NO to NO_2, or form alkyl nitrates

$RO_2 + NO \rightarrow RONO_2$,

$RO_2 + NO \rightarrow RO + NO_2$.

The photodissociation of NO_2 leads to O_3 formation. Further decomposition of RO yields the unsaturated C_4 carbonyls methacrolein (MACR) and methylvinyl ketone (MVK) plus formaldehyde (CH_2O). MACR and MVK account for about 60% of the first generation reaction products, alkyl nitrates contribute about 10%, whereas C_5 unsaturated aldehydes make up much of the rest (Pinho et al., 2005). These compounds readily react with OH and can also photo-dissociate. The reaction products include glycolaldehyde,

methylglyoxal and hydroxyacetone, and additional reactions with OH or photo-dissociation ultimately lead to CH_2O, CO and CO_2.

In low-NO conditions the yields of these compounds are reduced in favour of the formation of hydroperoxides (Miyoshi et al., 1994)

$RO_2 + HO_2 \rightarrow ROOH + O_2$.

For methyl hydroperoxide (CH_3OOH), a product of methane oxidation, the photo-dissociation frequencies and reaction rate coefficients with OH have been measured. In models the photochemical properties of CH_3OOH are often adopted for higher peroxides as the reactions of higher peroxides and higher peroxy radicals are largely unknown because the preparation of isoprene compounds in the laboratory is problematical. However, it is conceivable that photochemical OH production rates are larger for these more complex species.

Laboratory measurements

Experimental work by Hasson et al. (2004) indicates that peroxy radicals containing a carbonyl functional group may react with HO_2 to form OH at significant yield (α) of 0.4-0.67. This was confirmed by Jenkin et al. (2007) who obtained experimental evidence for OH formation (at $\alpha \approx 0.4$) in the reaction of acetylperoxy radicals with HO_2. In neither of these studies was the OH radical directly observed and product yields were derived by detection of secondary products. To verify that OH is formed at high yields in such reactions, we have conducted experiments in which OH was observed sensitively and

directly by laser induced fluorescence (LIF), the same method applied in the field studies reported here.

The experimental set up (see Dillon et al., 2006) employed pulsed laser photolysis of suitable precursor species to simultaneously generate RO_2 and HO_2. Experimental conditions were chosen so that HO_2 was generated in large excess to facilitate the kinetic analysis. Yields of OH were measured relative to the yield of OH in the reaction of HO_2 with NO, which is known to be 100% (Atkinson et al., 2007). A number of peroxy radicals was investigated, some with hydroxy subsitution (e.g. from ethanol or propanol) and some with carbonyl groups (e.g. from acetaldehyde or acetone). The organic peroxy radicals containing a carbonyl group all reacted with HO_2 to form OH at yields larger than 20%. The most efficient OH generation was observed in the reaction of HO_2 with $CH_3C(O)O_2$ ($\alpha \approx 0.5$), in good agreement with Hasson et al. (2004) and Jenkin et al. (2007). For $CH_3C(O)CH_2O_2$ (derived from acetone) a value of ~0.15 was obtained, much lower than obtained by Hasson et al (2004). OH formation was also observed in the reactions of HO_2 with RO_2 from benzaldehyde and butanone, albeit at relatively low yields (20-25 %) and associated with larger uncertainties. No evidence was found for OH formation from reaction of hydroxyl substituted peroxy radicals, though we note that Jenkin et al. (2007) report a yield of 0.2 for reaction of HO_2 with $HOCH_2O_2$ (not considered here).

These results confirm that organic peroxy radicals can react with HO_2 to regenerate OH under low-NO conditions. The yield of OH is strongly dependent on the structure of the peroxy radical and appears to be favoured by the presence of electron withdrawing substituents close to the peroxy group. We emphasise that detailed experimental (and

theoretical) investigations will be necessary to unravel the complexities of HO_2 + RO_2 reactions, especially in isoprene oxidation, and provide constraints on OH radical yields.

Modelling

Our atmospheric chemistry model (ACM) couples the 5th generation European Centre – Hamburg general circulation model, ECHAM5 (Roeckner et al., 2003, 2006) to the Modular Earth Submodel System, MESSy (Jöckel et al., 2006). The ACM computes atmospheric dynamics in a spectral framework using triangular truncation T42 (~2.8° horizontal resolution) and applies a relatively high number of 31 layers in the troposphere and lower stratosphere up to 10 hPa. Atmospheric chemistry is calculated by the MESSy set of modules also used by Pozzer et al. (2007), who evaluated the model by comparing the results with measurements of organic gases (see also www.messy-interface.org and http://www.atmos-chem-phys.net/special_issue22.html).

For detailed descriptions of the chemistry representation, atmosphere-biosphere interactions including parameterizations of micrometeorological processes and wet and dry deposition we refer to Ganzeveld et al. (2006), Kerkweg et al. (2006a,b, 2007), Tost et al. (2006a,b, 2007) and Sander et al. (2005). Global on-line calculated emissions of C_5H_8, $C_{10}H_{16}$ and other reactive VOCs from the vegetation are 0.59, 0.14 and 2.5×10^{15} gC/yr, respectively, and NO_x release from soils is 12.4×10^{12} gN/yr (canopy flux is 8.4×10^{12} gN/yr). A column model version has been used for sensitivity studies of atmosphere-biosphere exchange processes and tests against field measurements (Ganzeveld et al., 2002, 2004; Kuhn et al., 2007), and a box model version has been used

to study chemical mechanisms and help interpret the GABRIEL measurement data (Stickler et al., 2007).

The set of reactions used in the model base runs can be found in the electronic supplement of Sander et al. (2005). The original Mainz Isoprene Mechanism (MIM) was developed by Pöschl et al. (2000) and was implemented according to von Kuhlmann et al. (2004) (Sander et al., 2005). For the present study it has been extended to MIM2 from 16 to 69 isoprene related species and from 44 to 181 reactions and tested against the Master Chemical Mechanism (MCM) (Jenkin et al., 1997, 2003; Saunders et al., 2003; Pinho et al., 2005) (see http://mcm.leeds.ac.uk/MCM/). In contrast to MIM, MIM2 does not lump first generation oxidation products and closely follows MCM in the representation of oxidation reactions by OH, O_3 and NO_3 as well as the formation of alkyl nitrates, hydroperoxides and diols (D. Taraborrelli, manuscript in preparation).

In MIM2+ we have further enhanced OH recycling by assuming that several OH radicals can be formed through all reactions of first generation RO_2 from isoprene oxidation with HO_2, in analogy to the Hasson et al. (2004) reactions (T. Butler, manuscript in preparation). Possible additional explanations include stronger than anticipated photodissociation of organic peroxy radicals and peroxides (e.g. Frost et al., 1999; Thornton et al., 2002; Matthews et al., 2005) (in MIM and MIM2 we apply the photo-dissociation rate of methyl hydroperoxide to all organic peroxides, whereas peroxy radicals do not photo-dissociate). This recycles in total 40-80% of the OH consumed in the degradation of isoprene for the conditions during GABRIEL, assuming that 2-4 OH radicals are formed, respectively. Note that HO_2 + RO_2 reactions are unlikely to recycle more OH than 60% directly, and some of the artificial OH production assumed here may

actually be due to other sources. Possibly the overall OH yield is a combination of factors all working in the same direction, but with none being dominant.

Figures S2 and S3 extend Figure 2 and compare measurements (circles) of OH and HO_2/OH ratios with model results (background). They show that MIM underestimated OH in the BL by up to a factor of 5-10, whereas in the free troposphere the agreement was better. Note that at about 2-3 km altitude OH levels were slightly enhanced in early October by the long-distance transport of O_3 in a dilute biomass burning plume from southern Brazil (Petersen et al., 2007; Stickler et al., 2007).

The MIM2 mechanism leads to a substantial improvement of OH concentrations and HO_2/OH ratios. However, OH in the BL is still more than a factor of two too low, whereas with MIM2+ much better agreement is achieved. Figure S4 shows the model calculated mean OH concentrations for the three mechanisms, indicating largest changes over the forested continents in the tropics. Neither MIM2 nor MIM2+ produce significantly more OH in high-NO regions and over the oceans compared to the original MIM scheme, and all three mechanisms produce realistic ozone distributions. Only the MIM2+ mechanism eliminates the unrealistically low OH concentrations over the tropical forests, and good agreement is obtained for the BL and free troposphere both over land and the ocean.

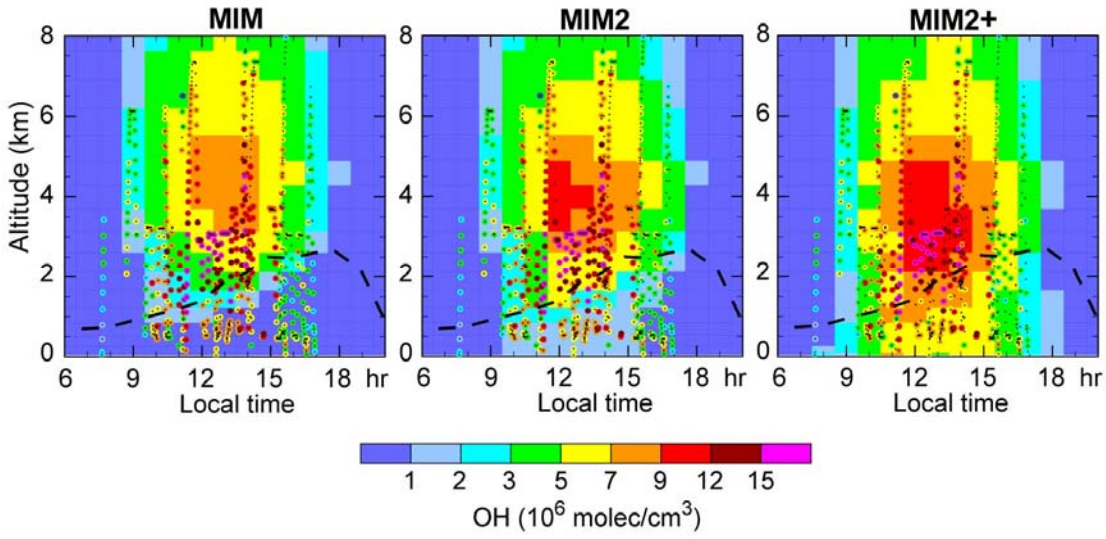

Figure S2. Model calculated (background) and measured (circles) daytime OH concentrations over Suriname in October 2005. The black dashed lines delineate the upper bound of convective mixing. Model results were obtained with the MIM, MIM2 and MIM2+ mechanisms. MIM is the original isoprene oxidation mechanism, MIM2 the mechanism extended to closely follow the MCM, and MIM2+ with additional OH produced from reactions of HO_2 with organic peroxy radicals.

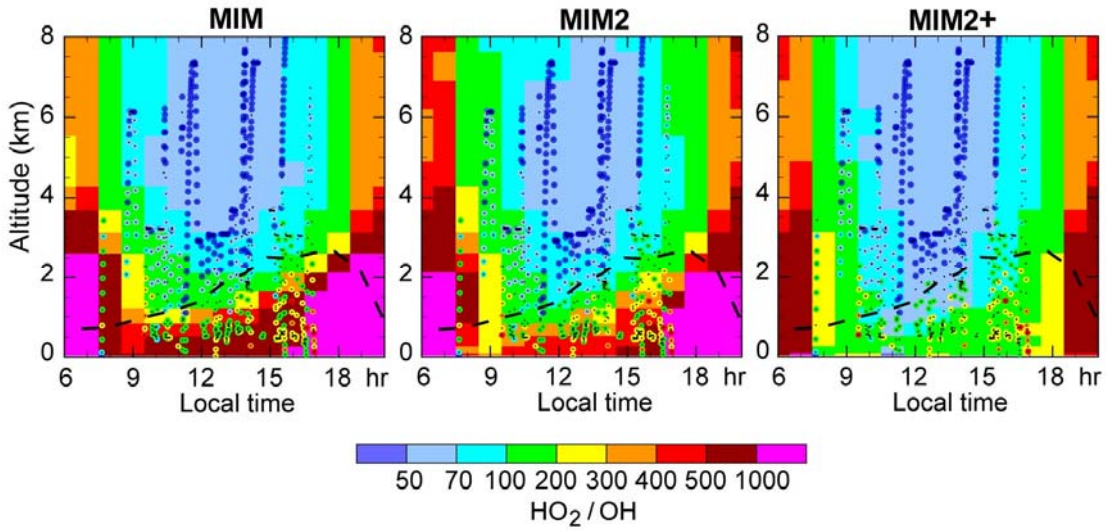

Figure S3. As Figure S2 but showing model calculated (background) and measured (circles) daytime HO_2/OH ratios over Suriname in October 2005.

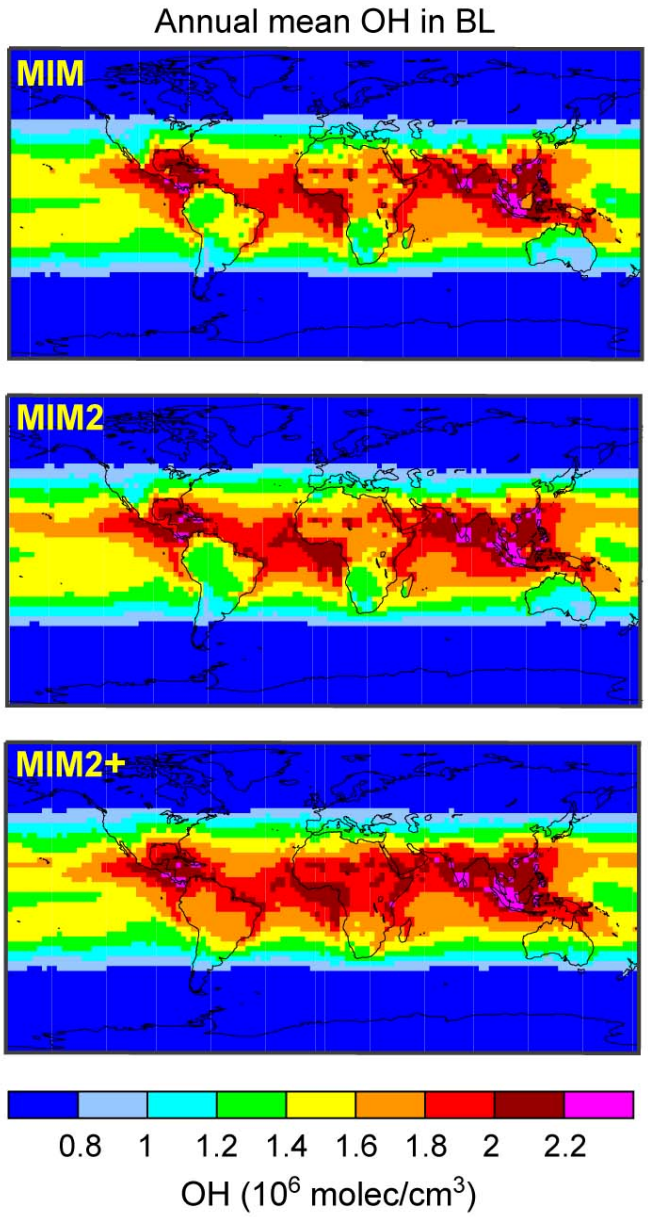

Figure S4. Model calculated annual mean OH in the boundary layer using the MIM, MIM2 and MIM2+ mechanisms. The OH differences are largest over the forests in low-NO air in the Southern Hemisphere, i.e. in South America, Africa and Australia. Note that during periods of strong biomass burning NO is enhanced in these regions, so that the effects on OH are smaller than during more pristine environmental conditions.

References

Andreae, M. O. *et al*. Transport of biomass burning smoke to the upper troposphere by deep convection in the equatorial region. *Geophys. Res. Lett*. **28**, 951-954 (2001).

Atkinson, R. *et al*., IUPAC Subcommittee for gas kinetic data evaluation. Evaluated kinetic data: http://www.iupac-kinetic.ch.cam.ac.uk/ (2007).

Carter, W. P. L. & Atkinson, R. Development and evaluation of a detailed mechanism for the atmospheric reactions of isoprene and NO_x. *Int. J. Chem. Kin.* **28**, 497-530.

Colomb, A. *et al*. Airborne measurements of trace species in the upper troposphere over Europe: the impact of deep convection. *Environ. Chem.* **3**, 244-259 (2007).

Crutzen, P.J. *et al*. High spatial and temporal resolution measurements of primary organics and their oxidation products over the tropical forests of Surinam. *Atmos. Environ*. **34**, 1161-1165 (2000).

Dillon, T. J., Horowitz, A., Hölscher, D. & Crowley, J. N. Reaction of HO with hydroxyacetone ($HOCH_2C(O)CH_3$): rate coefficients and mechanism *Phys. Chem. Chem. Phys.* **8**, 236-246 (2006).

Fischer, H. *et al*., Model simulations and aircraft measurements of vertical, seasonal and latitudinal O_3 and CO distributions over Europe. *Atmos. Chem. Phys*. **7**, 339-348 (2006).

Formenti, P. *et al*. Saharan dust in Brazil and Suriname during the Large-Scale Biosphere-Atmosphere Experiment in Amazonia (LBA) - Cooperative LBA Regional Experiment (CLAIRE) in March 1998. *J. Geophys. Res*. **106**, 14919-14934 (2001).

Frost, G.J., Ellison, G. B. & Vaida, V. Organic peroxy radical photolysis in the near-infrared: Effects on tropospheric chemistry. *J. Phys. Chem*. **103**, 10169-10178 (1999).

Ganzeveld, L. N. *et al*. Global soil-biogenic NO_x emissions and the role of canopy processes. *J. Geophys. Res*. **107**, doi: 10.1029/2001JD001289 (2002).

Ganzeveld, L. N. & Lelieveld, J. Impact of Amazonian deforestation on atmospheric chemistry. Geophys. Res. Lett. **31**, L06105, doi: 10.1029/2003GL019205 (2004).

Ganzeveld, L.N. *et al*. Technical note: Anthropogenic and natural offline emissions and the online emissions and dry deposition (EMDEP) submodel of the Modular Earth Submodel System. *Atmos. Chem. Phys*. **6**, 5457-5483 (2006).

Hasson, A. S., Tyndall, G. S. & Orlando, J. J. A product yield study of the reaction of HO_2 radicals with ethyl peroxy ($C_2H_5O_2$) acetyl peroxy ($CH_3C(O)O_2$), and acetonyl peroxy ($CH_3C(O)CH_2O_2$) radicals. *J. Phys. Chem*. **108**, 5979-5989 (2004).

Jenkin, M. E., Saunders, S. M. & Pilling, M. J. The tropospheric degradation of volatile organic compounds: a protocol for mechanism development. *Atmos. Environ.* **31**, 81-104 (1997).

Jenkin, M. E., Saunders, S. M., Wagner, V. & Pilling, M. J. MCM v3 (Part B): tropospheric degradation of aromatic volatile organic compounds. *Atmos. Chem. Phys*. **3**, 191-193 (2003).

Jenkin, M.E., Hurley, M. D. & Wallington, T. J. Investigation of the radical product channel of the $CH3COO_2 + HO_2$ reaction in the gas phase. *Phys. Chem. Chem. Phys*. **9**, 3149-3162 (2007).

Jöckel, P. *et al*. The atmospheric chemistry general circulation model ECHAM5/MESSy, Consistent simulation of ozone from the surface to the mesosphere. *Atmos. Chem. Phys*. **6**, 5067-5104 (2006).

Kerkweg, A., Sander, R., Tost, H. & Jöckel, P. Technical Note: Implementation of prescribed (OFFLEM), calculated (ONLEM), and pseudo-emissions (TNUDGE) of chemical species in the Modular Earth Submodel System (MESSy). *Atmos. Chem. Phys*. **6**, 3603-3609 (2006a).

Kerkweg A. *et al*. Technical Note: An implementation of the dry removal processes DRY DEPosition and SEDImentation in, the Modular Earth Submodel System (MESSy) *Atmos. Chem. Phys*. **6**, 4617-4632 (2006b).

Kerkweg, A., Sander, R. Tost, H., Jöckel, P. & Lelieveld, J. Technical Note: simulation of detailed aerosol chemistry on the global scale using MECCA-AERO. *Atmos. Chem. Phys*. **7**, 2973-2985 (2007).

Kuhn, U. *et al*. Isoprene and monoterpene fluxes from Central Amazonian rainforest inferred from tower-based and airborne measurements, and implications on the atmospheric chemistry and the local carbon budget. *Atmos. Chem. Phys*. **7**, 2855-2879 (2007).

Matthews, J., Sinha, A. & Francisco, J. S. The importance of weak absorption features in promoting tropospheric radical production. *Proc. Nat. Acad. Sci*. **102**, 7449-7452 (2005).

Miyoshi, A. Hatakeyama, S. &Washida, N. OH-radical initiated photooxidation of isoprene: An estimate of global CO production. *J. Geophys. Res*. **99**, 18779-18787 (1994).

Nurmohamed, R. J. & Naipal, S. Variability of rainfall in Suriname and the relation with ENSO-SST and TA-SST. *Adv. Geosc*. **6**, 77-82 (2006).

Paulson, S. E., Flagan, R. C. & Seinfeld, J. H. Atmospheric photo-oxidation of isoprene: Part 1. The hydroxyl radical and ground state atomic oxygen reactions. *Int. J. Chem. Kin*. **24**, 79-101.

Peters, W. *et al*. Tropospheric ozone over a tropical Atlantic station in the Northern Hemisphere: Paramaribo, Surinam (6°N, 55°W). *Tellus* **56B**, 21-34 (2004).

Petersen, A. K., Warneke, T., Lawrence, M. G., Notholt, J. & Schrems, O. First ground-based FTIR observations of the seasonal variation of carbon monoxide in the tropics. *Geophys. Res. Lett*. (in press).

Pinho, P. G., Pio, C. A. & Jenkin, M. E. Evaluation of isoprene degradation in the detailed tropospheric chemical mechanism, MCM v3, using environmental chamber data. *Atmos. Environ*. **39**, 1303-1322 (2005).

Pöschl, U., von Kuhlmann, R., Poisson, N. & Crutzen, P. J. Development and intercomparison of condensed isoprene oxidation mechanisms for global atmospheric modelling. *J. Atmos. Chem*. **37**, 29-52 (2000).

Pöschl, U. *et al*. High acetone concentrations throughout the 0-12 km altitude range over the tropical rainforest in Surinam. *J. Atmos. Chem*. **38**, 115-132 (2001).

Pozzer, A. *et al*. Simulating organic species with the global atmospheric chemistry general circulation model ECHAM5/MESSy1: a comparison of model results with observations *Atmos. Chem. Phys*. **7**, 2527-2550 (2007).

Roeckner, E. *et al*. The atmospheric general circulation model ECHAM5. PART I: Model description, Max Planck Institute for Meteorology, MPI-Report 349, http://www.mpimet.mpg. de/fileadmin/publikationen/Reports/max scirep 349.pdf (2003).

Roeckner, E. *et al*. Sensitivity of simulated climate to horizontal and vertical resolution in the ECHAM5 atmosphere model. *J. Climate* **19,** 3771-3791 (2006).

Sander, R., Kerkweg, A., Jöckel, P. & Lelieveld, J. Technical Note: The new comprehensive atmospheric chemistry module MECCA. *Atmos. Chem. Phys*. **5**, 445-450 (2005).

Saunders, S. M., Jenkin, M. E., Derwent, R. G. & Pilling, M. J. Protocol for the development of the Master Chemical Mechanism, MCM v3 (Part A): tropospheric degradation of non-aromatic volatile organic compounds. *Atmos. Chem. Phys*. **3**, 161-180 (2003).

Stickler, A. *et al*. Influence of summertime deep convection on formaldehyde in the middle and upper troposphere over Europe. *J. Geophys. Res*. **111**, D14308, doi:10.1029/2005JD007001 (2006).

Stickler, A. *et al*. Chemistry, transport and dry deposition of trace gases in the boundary layer over the tropical Atlantic Ocean and the Guyanas during the GABRIEL field campaign. *Atmos. Chem. Phys*. **7**, 3933-3956 (2007).

Thornton, J. A. *et al*. Ozone production rates as a function of NO_x abundances and HO_x production rates in the Nashville urban plume. *J. Geophys. Res.* **107**, D12, doi: 10.1029/2001JD000932 (2002).

Tost, H., Jöckel, P., Kerkweg, A., Sander, R. & Lelieveld, J. Technical Note: A new comprehensive SCAVenging submodel for global atmospheric chemistry modelling. *Atmos. Chem. Phys*. **6**, 565-574 (2006a).

Tost, H., Jöckel, P. & Lelieveld, J. Influence of different convection parameterisations in a GCM. *Atmos. Chem. Phys*. **6**, 5475-5493 (2006b).

Tost, H. *et al.* Global cloud and precipitation chemistry and wet deposition: tropospheric model simulations with ECHAM5/MESSy1. *Atmos. Chem. Phys*. **7**, 2733-2757 (2007).

von Kuhlmann, R., Lawrence, M. G. Pöschl, U. & Crutzen, P. J. Sensitivities in global scale modelling of isoprene. *Atmos. Chem. Phys*. **4**, 1-17 (2004).

Warneke, C. *et al*. Isoprene and its oxidation products methyl venyl ketone, methacrolein, and isoprene related peroxides measured online over the tropical rain forest of Surinam in March 1998. *J. Atmos. Chem*. **38**, 167-185 (2001).

Williams, J. *et al*. An atmospheric chemistry interpretation of mass scans obtained from a proton transfer mass spectrometer flown over the tropical rainforest of Surinam. *J. Atmos. Chem.* **38**, 133-166 (2001a).

Williams, J. *et al*. Influence of the tropical rain forest on atmospheric CO and CO_2 as measured by aircraft over Surinam, South America. *Chemosphere - Glob. Change Sci*. **3**, 157-170 (2001b).

Williams, J., Yassaa, N., Bartenbach, S. & Lelieveld, J. Mirror image hydrocarbons from Tropical and Boreal forests. *Atmos. Chem. Phys*. **7**, 973-980 (2007).